RJC

RASĀYAN ***J. Chem.***
Vol. 9 | No. 4 |751 - 761 | October - December | 2016
ISSN: 0974-1496 | e-ISSN: 0976-0083 | CODEN: RJCABP
http://www.rasayanjournal.com
http://www.rasayanjournal.co.in

THE ELECTROSTATIC PROPERTIES OF 1,2-DIMETHYL-3-NITROBENZENE COMPOUND: *ab initio* CALCULATION AND X-RAY CHARGE DENSITY ANALYSIS

N. Boubegra, Y. Megrouss, N. Boukabcha, A. Chouaih* and F. Hamzaoui

Laboratory of Technology and Solid Properties (LTPS), Abdelhamid Ibn Badis University of Mostaganem, 27000 Mostaganem, Algeria
*E-mail : achouaih@gmail.com

ABSTRACT

Electrostatic atomic and molecular properties of the 1,2-dimethyl-3-nitrobenzene are derived from both experimental data and *ab initio* theoretical investigation. The molecular dipolar moment obtained by both methods is around 6 Debye and its orientation shows clearly the direction of the intra-molecular charge transfer. The obtained net atomic charges and the derived electrostatic potential show that the electronegative potential is located on the side on the nitro group region whereas the electropositive potential is on the side of the methyl groups. The experimental electrostatic potential is derived from high-resolution single-crystal X-ray diffraction data. The crystallographic investigations are carried out using the multipolar model of Hansen and Coppens in order to take into account the non-spherical part of the atomic electron charge density distribution. In addition to the structural analysis, a thermal motion analysis is carried out in terms of rigid blocks in order to improve the accuracy of obtained results. The experimental results are compared to *ab initio* theoretical Hartree-Fock (HF) and density functional theory (DFT) predictions, using two different large basis sets. Both DFT and HF calculations gave a molecular dipole moment in good agreement with the extracted one from the X-ray diffraction data (value of 6.57 D). The theoretical investigations are found to reproduce well the experimental molecular electrostatic potential. In the present work, the intermolecular hydrogen bonds are also subjected to a detailed experimental topological analysis.

Keywords: molecular structure, multipolar refinement, hydrogen bonding, thermal motion, dipole moment.

INTRODUCTION

The organic hydrocarbons having one or more NO_2 groups bonded via nitrogen to the carbon framework are considered as important chemical compounds from an industrial point of view. [1] They are widely used as intermediate in organic synthesis. The investigated molecule the 1,2-dimethyl-3-nitrobenzene known under the commercial acronym 3-Nitro-o-xylenes is a very useful intermediate for manufacturing of agrochemicals and pharmaceutical products. It is known that the reactional mechanism and the biological activities for such molecules are directly linked to their electrostatic environment. [2,3] That is why the research on electrostatic properties of 3-Nitro-o-xylenes molecule are of great interest. This let us to describe accurately the electrophile and the nucleophile regions in this molecule. In this context, our contribution to this field focuses on the study of the molecular electrostatic potential around the molecule and we provide some other electrostatics properties such as the net atomic charges and the molecular dipole moment. In the present work both experimental and theoretical investigations are presented.

The X-ray crystal data were taken from the web site of International Union of Crystallography. The used parameters in the current study are summarized in Table-1. The crystal structure has been described in a previous work by Sparkes*et.al*.[4] The compound crystallizes in the $P2_12_12_1$ space group, with four molecules in the unit cell. The general feature of the structure consists of dimethyl substituted ring benzene connected to NO_2 group as shown in Figure-1. The molecule does not occur in a same plane, the

NO_2 group is rotated out of the benzene plane ring by an angle of 45°. In the crystal the molecules are connected via hydrogen weak interactions.

The previous crystallographic investigation presented by Sparkes et al. is based on atomic spherical charge density model which does not take into account the non-spherical charge density existing along the chemical bound. So in order to improve the accuracy of the structural parameters and to bring out the experimental charge density around the molecule our crystallographic investigation have been carried out using the multipolar charge density model of Hansen and Coppens.[5] On the other hand, a special care was reserved to the treatment of the Hydrogen atoms. The anisotropic motion of the H atoms was derived from a thermal motion analysis carried on the molecule using the rigid block bond test as described by Hirshfield *et al.*[6,7]

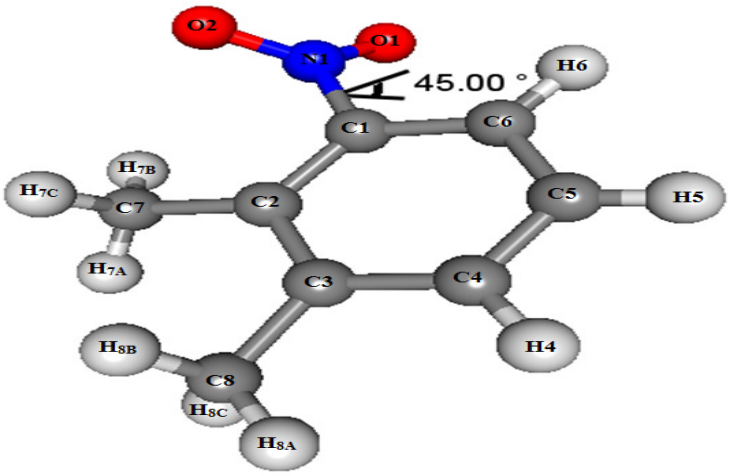

Fig.-1: Optimal structure of the title compound.

In the present work, the experimental results are compared to ab initio theoretical Hartree-Fock (HF) and density functional theory (DFT) predictions. In each case the geometry optimization was performed starting from the molecular geometry found in the experimental X-ray investigation. The DFT method was based on the Becke-Lee-Yang-Part's three-parameter hybrid functional (B3LYP) parameters and HF approximation was carried with the basis set 6-31G(d,p). [8-14] All the theoretical calculations here were performed using the Gaussian 09 and the Gauss-View molecular visualization programs.[15,16] The obtained results are in good agreement with those derived from the experimental investigation. In addition, the intermolecular hydrogen bonds have been subjected to a detailed experimental topological analysis. The experimental investigation based on the multipolar model led to a faithful description of the electron charge density distribution in the crystal. The electrostatic potential around the molecule is also calculated so as to describe the electrostatic environment created around the molecule.

EXPERIMENITAL

Crystallographic investigation

The crystallographic results presented by Sparkes *et al.* based on spherical atomic model was improved by taking into account in the refinement the non-spherical electron charge density existing along the chemical bound as described in the multipolar model of Hansen and Coppens.[5] In this last model the molecular electron density is described as a superposition of non-spherical pseudo-atoms modeled using a multipole expansion as:

$$\rho_{atom}(\vec{r}) = \rho_c(\vec{r}) + P_v\kappa'^3\rho_v(\kappa'\vec{r}) + \sum_{l=0}^{lmax}\sum_{m=-l}^{m=+l}\kappa''\,R_l(\kappa''\vec{r})P_{lm}Y_{lm}\left(\frac{\vec{r}}{r}\right) \quad (1)$$

Where,ρ_c and ρ_v are spherically averaged Hartree-Fock core and valence density respectively, with ρ_v being normalized to one electron; $Y_{lm\pm}$ are the spherical harmonic angular functions that are modulated by the Slater-type radial functions; N_l is a normalization factor. The values for parameters $n = n_l$ and is chosen according to the rules suggested by Coppens (1997).[17] In practice, the expansion and contraction of the valence shell depend on two charge density variables, the population parameter and a kappa parameter; they are added to the conventional parameters of structure analysis. The population parameters P_v and $P_{lm}$are floated along with k' and k''during the refinement, the summation over m in Eq. (1) includes ±*l*, so that for each one, 2*l* +1 functions are included. The aspheric charge density is described at the octupole level (l =3) for the atoms C, N, and O and at the dipole levels (l = 1 or 2) for hydrogen atoms not involved and involved in strong H bonds, respectively. Charge densities of all hydrogen are considered to have cylindrical symmetry along the corresponding hydrogen-heavy atom bond.

The refinements were performed using the MOPRO program in which the Hansen- Coppens multipole formalism is implemented. [18] The least-square method is used to refine the crystal structure against F^2 using atomic anisotropic thermal parameters for all non-hydrogen atoms. The H atoms are located from a difference Fourier map and included in the refinement with the isotropic temperature factor of the carrier atom. After the thermal motion analysis in terms of the rigid body bond test, the anisotropic temperature factors for the hydrogen atoms are introduced. The accuracies of results are significantly improved: the final refinement R factor decreases to 1%. The crystallographic details are given in Table-1.

Table-1: Crystal data and structure refinement details.

Compound empirical formula	1,2-dimethyl-3-nitrobenzene C8H9NO2
Temperature/K	277(2)
Crystal system, space group	Orthorhombic, $P2_12_12_1$
Unit cell dimension	
a/Å	3.9338(5)
b/Å	14.022(3)
c/Å	14.126(3)
Wavelength/Å	0.71073
Z, calculated density/g/cm^{-3}	4/1.289
Observed Reflections	824

Least-square multipole refinement factors: N is the Number of Refined Parameters.
The atomic scattering factors come from the international tables for X-ray crystallography.

	N	$R = \Sigma\|Fo\| - \|Fc\|/\Sigma\|Fo\|$
Spherical Model [3]	126	3.5 %
Multipolar Model	213	1.0 %

Thermal Motion Analysis

The molecular thermal motion analysis has been performed using the THMA11 program. [6] This analysis the molecule is considered as a rigid-body and its motion related to a molecular frame can be described by three tensors, *T*for the translation, *L*for the liberation and S when taking into account the correlation between translation and liberation. These tensors are obtained by a least-square fit refinement using the observed non-H atomic (C, N, and O atoms) thermal motion parameters obtained from X-ray refinement and are reported in Table-2. In the rigid body bond model, the bonded pairs of the non-H atoms are assumed having the differences between the mean-square displacement amplitudes (MSDAs) along the interatomic directions $\Delta \leq 10.10^{-4}$Å^2. [19] For all pairs of atoms in the molecule, the MSDAs Δ_{AB} in the AB direction have been calculated and reported in Table-3.

In the general treatment of the molecular thermal motion in terms of rigid-body (TLS), the calculated anisotropic thermal parameters are given in the Trueblood notation such as:

$$U_{IJ} = T_{IJ} + G_{IJKL}L_{KL} + H_{IJKL}SKL + D^2\Omega^2_{ninj} \quad (2)$$

Where G, and D are geometrical parameters. The last term in equation (2) is related to any additional intra-libration (Ω) around a chosen axis. The rigid-body fit suggests one independent liberation axis around the bond C(1)–N(1). The thermal motion of the H atoms takes into account two contributions. The first is due to the rigid molecular motion and the second to the C–H vibrations.[20,21]The T, L, and S tensors obtained from the least-square fitting are given in Table-4. The C–H bond frequencies of the molecule were taken from Baert et al. [22]The results of the thermal motion parameters of the H atoms are summarized in Table-5. Ellipsoids of the different atoms representing their thermal motion described above are shown in Figure-2 using MoProviewer program.[23]

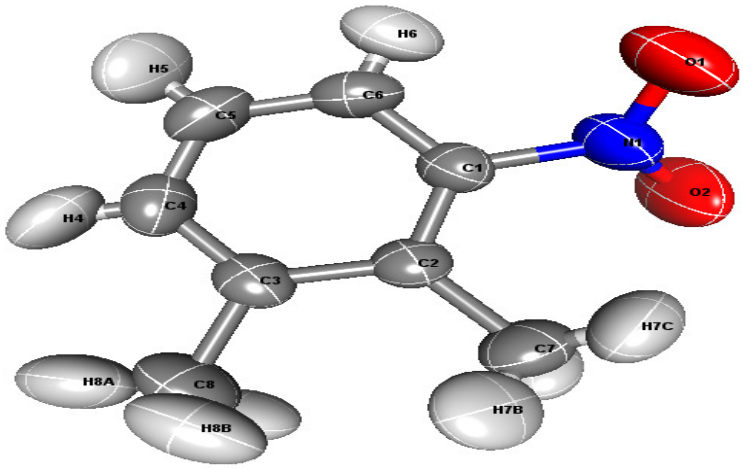

Fig.-2: Thermal ellipsoids are shown for the 50% probability level.

Table-2: Atomic displacement parameters in units of Å^2.

Atoms	U11	U22	U33	U12	U13	U23	
O1	0.1320	0.0632	0.0985	0.0281	-0.0148	-0.0221	*Observed*
	0.1319	0.0612	0.0963	0.0258	-0.0111	-0.0226	*Calculated*
	0.0001	0.0020	0.0022	0.0023	-0.0037	0.0005	*Difference*
O2	0.1690	0.0958	0.055	0.0282	-0.0239	-0.0143	*Observed*
	0.1550	0.0898	0.0559	0.0206	-0.0242	-0.0195	*Calculated*
	0.0140	0.0060	-0.0009	0.0076	0.0003	0.0052	*Difference*
N1	0.0864	0.0540	0.0627	0.0089	-0.0100	-0.0102	*Observed*
	0.1047	0.0607	0.0626	0.0155	-0.0140	-0.0139	*Calculated*
	-0.0183	-0.0067	0.0001	-0.0066	0.0040	0.0037	*Difference*
C1	0.0557	0.0476	0.048	0.0036	-0.0079	-0.0025	*Observed*
	0.0526	0.0454	0.0488	0.0061	-0.0112	0.0017	*Calculated*
	0.0031	0.0022	-0.0008	-0.0025	0.0033	-0.0042	*Difference*
C2	0.0507	0.0460	0.0488	0.0064	-0.0052	0.0050	*Observed*
	0.0460	0.0457	0.0471	0.0064	-0.0057	0.0047	*Calculated*
	0.0047	0.0003	0.0017	0.0000	0.0005	0.0003	*Difference*
C3	0.0540	0.0485	0.0569	0.0096	-0.0130	-0.0039	*Observed*
	0.0530	0.0503	0.0542	0.0077	-0.0104	-0.0043	*Calculated*
	0.0010	-0.0018	0.0027	0.0019	-0.0026	0.0004	*Difference*
C4	0.0710	0.0753	0.0474	0.0159	-0.0040	-0.0044	*Observed*
	0.0749	0.0763	0.0475	0.0136	-0.0006	-0.0025	*Calculated*
	-0.0039	-0.0010	-0.0001	0.0023	-0.0034	-0.0019	*Difference*
C5	0.0700	0.0813	0.0542	0.0042	0.0045	0.0188	*Observed*
	0.0724	0.0791	0.0570	0.0053	0.0055	0.0183	*Calculated*

	-0.0024	0.0022	-0.0028	-0.0011	-0.0010	0.0005	*Difference*
C6	0.0652	0.0508	0.0674	-0.0005	-0.0058	0.0133	*Observed*
	0.0575	0.0528	0.0658	-0.0009	-0.0093	0.0141	*Calculated*
	0.0077	-0.0020	0.0016	0.0004	0.0035	-0.0008	*Difference*
C7	0.0720	0.0649	0.0649	0.0036	0.0071	0.0156	*Observed*
	0.0799	0.0665	0.0670	0.0074	0.0127	0.0198	*Calculated*
	-0.0079	-0.0016	-0.0021	-0.0038	-0.0056	-0.0042	*Difference*
C8	0.0890	0.0518	0.0977	0.0041	-0.0154	-0.0149	*Observed*
	0.0871	0.0516	0.0993	0.0047	-0.0203	-0.0153	*Calculated*
	0.0019	0.0002	-0.0016	-0.0006	0.0049	0.0004	*Difference*

Table-3: Matrix for differences in MSDA (mean square displacements of atoms): values listed are 10^4 MSDAs for column atom minus that for row atom.

Atoms	C8	C7	C6	C5	C4	C3	C2	C1	N1
O1									-35
O2									21
N1								-51	
C1			-4				-6		
C2		9				7			
C3	10				0				
C4				18					
C5			-6						

Table-4: Rigid body vibration parameters of the T, L, and S tensors

T (Å^2)	L (rad^2)	S (Å.rad)
$\begin{pmatrix} 0.04779 & 0.00104 & 0.00101 \\ & 0.04866 & 0.01025 \\ & & 0.03980 \end{pmatrix}$	$\begin{pmatrix} 0.00753 & -0.00271 & 0.00141 \\ & 0.00825 & -0.00210 \\ & & 0.00814 \end{pmatrix}$	$\begin{pmatrix} 0.00078 & -0.00082 & -0.00242 \\ 0.00025 & 0.00171 & 0.00593 \\ -0.00090 & -0.00378 & -0.00249 \end{pmatrix}$

Table-5: Thermal vibration parameters for the H atoms calculated from the T L S group tensors

Atoms	U11	U22	U33	U12	U13	U23
H4	0.1188	0.1059	0.0539	0.0242	0.0062	-0.0138
H5	0.1082	0.112	0.0736	0.0054	0.0227	0.0350
H6	0.0785	0.0543	0.0975	-0.0077	-0.0138	0.0204
H7A	0.1072	0.0742	0.0636	0.0124	0.0026	0.0272
H7B	0.0775	0.0696	0.1056	-0.0033	0.0179	0.0272
H7C	0.1026	0.0884	0.0704	0.0160	0.0305	0.0183
H8A	0.1262	0.0695	0.1083	0.0149	-0.025	-0.0366
H8B	0.0887	0.057	0.1327	-0.0109	-0.0295	-0.0110
H8C	0.0933	0.0456	0.1137	0.0099	-0.0148	-0.0039

RESULTS AND DISCUSSION

Structural analysis

The crystal structure has already been described by Sparkes & al. and no significant differences were found here. The theoretical part leads also to the same conclusion. The values of the structure bond lengths and bond angles are listed in Tables-6 and 7 respectively. The tables provide a comparison between the experimental X-ray values (first column) and the theoretical ones (second and third columns). The DFT method was based on the Becke-Lee-Yang-Part's three-parameter hybrid functional

(B3LYP) parameters and HF approximation was carried with the 6-31G(d,p) basis set. One can observe the good agreement between the different values which are closer to expended range found in literature. One can also consider the calculated geometric parameters as a good approximation and can be used as a starting point to calculate other parameters, such as vibrational wavenumbers.

Electron Density Maps

Though X-ray charge-density analysis is now rather routinely used to derive solid-state electrostatic moments, the moments from an aspherical-atom multipole refinement are sensitive to the details of the refinement procedure. This enables the mapping of the electron density distribution using Difference Fourier Synthesis to observe the experimental charge density deformation of the molecule. Figure-3 shows the electron charge density distribution in two different planes of the molecule: the first plane (a) formed by the electro-donor group (benzene ring), and the second plane (b) containing the electro-acceptor group (NO_2). In these figures, we can observe the absence of the density on the atomic sites and the appearance of all bond density peaks as expected in literature. These maps consist on a first confirmation concerning the high quality of the data sets and the efficiency of the used model of Hansen and Coppens.[5]

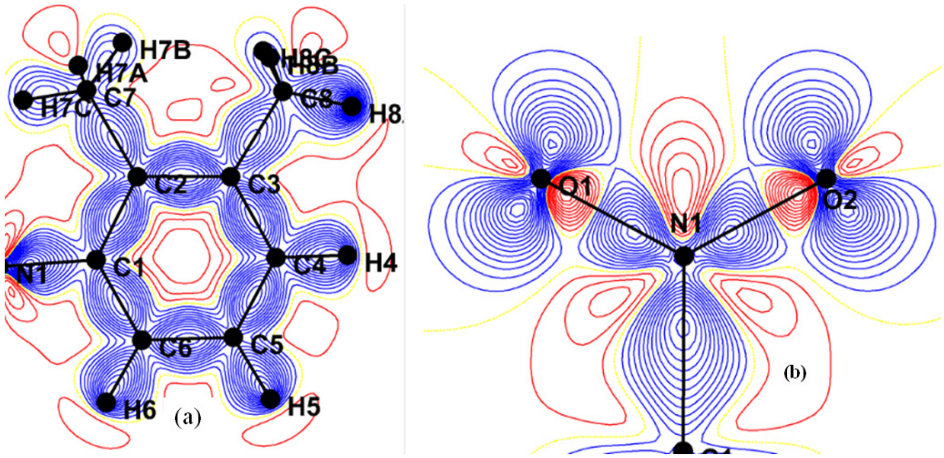

Fig.-3: Deformation Density Map with a Contour Interval of 0.05 e.Å^{-3}, positive density in blue, and negative density in red: (a) benzene ring plane, (b) the NO2 group.

Hydrogen bonding

Intermolecular hydrogen bonding plays an important role in the cohesion of solid condensed phases. The presence of intramolecular hydrogen bonds leads to an increase of the melting and boiling points. The presence of this type of connections (intramolecular bonds) can block the molecule in a particular conformation. In the case of aspirin, it prevents rotation of the functional groups which remain in the plane of the benzene ring; this intramolecular stress also makes the hydrogen less sensitive to interactions with other molecules. This reduces the available against an exchange with a basic molecule. Hydrogen bonding is capable of transferring H^+ ions between the molecules it binds. This property is very important since it is responsible for the reactivity of aqueous media. Without it, they would be inert and life would not be possible, because biological molecules constantly need to respond to remain active.

The exploration of the molecular environment within the unit cell gives rise to two types of interactions: As shown in Figures-4, 5 and 6, the first concerns a strong intramolecular or intermolecular hydrogen bond as O2–H7…C7 and C4–H4…O2 the second involved a weak intermolecular hydrogen bond responsible for the crystal package defined by the sites C5–H5...O1and C7–H7B...O1. Table-8 gives the description of the hydrogen bonds spotted in the crystal structure.

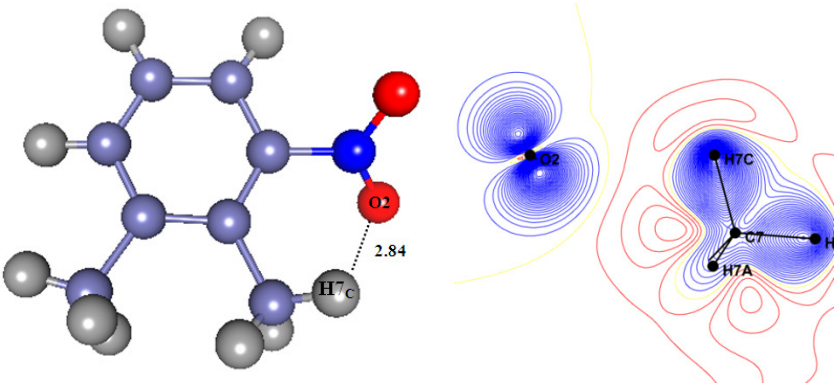

Fig.-4: Deformation density map of intramolecular hydrogen bond O2…H7...C7 with a contour interval of 0.05 e.Å^{-3}, positive density in blue and negative density in red.

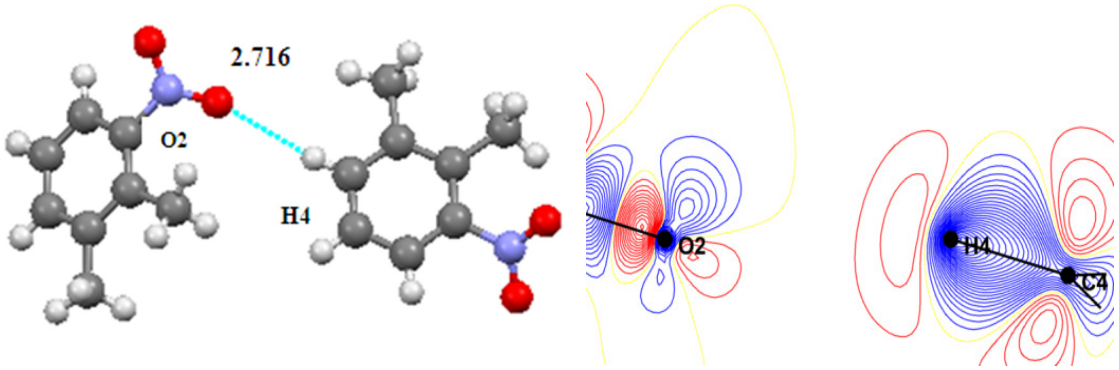

Fig.-5: Deformation density map in the plane of the intermolecular hydrogen bond C4…H4…O2 with a contour interval of 0.05 e.Å^{-3}, positive density in blue and negative density in red.

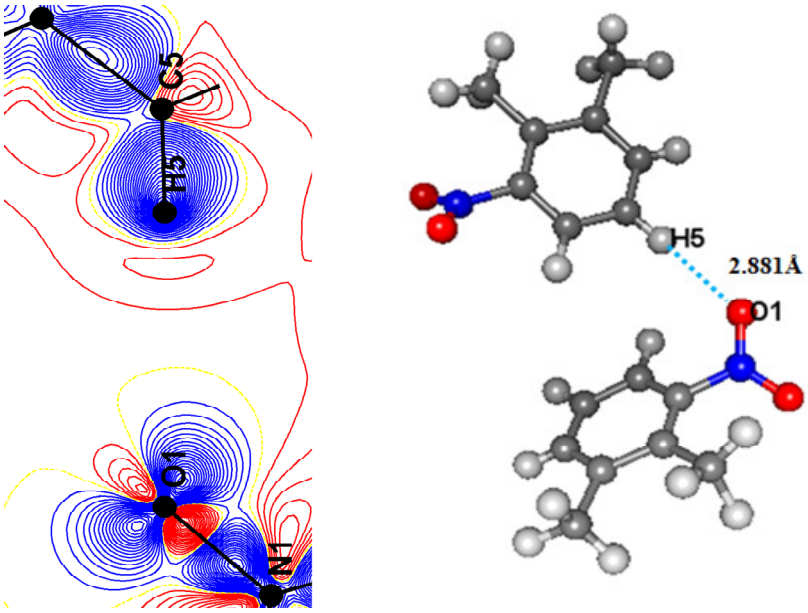

Fig.-6: Deformation density map in the plane of the intermolecular hydrogen bond C5…H4…O1 with a contour interval of 0.05 e.Å^{-3}, positive density in blue and negative density in red.

Table-6: Bond lengths of 12-dimethyl-3-nitrobenzene in units of Å

Atom 1	Atom 2	Distances		
		X-ray	DFT	HF
O1	N1	1.2156	1.2315	1.1945
O2	N1	1.2084	1.2322	1.1942
N1	C1	1.4723	1.4743	1.4621
C1	C2	1.3908	1.4073	1.3925
C1	C6	1.3813	1.3960	1.3847
C2	C3	1.3982	1.4154	1.4041
C2	C7	1.5077	1.5110	1.5141
C3	C4	1.3840	1.3991	1.3874
C3	C8	1.5082	1.5126	1.5136
C4	C5	1.3671	1.3941	1.3843
C5	C6	1.3660	1.3866	1.3759
C4	H4	0.9502	1.0865	1.0757
C5	H5	0.9504	1.0850	1.0744
C6	H6	0.9506	1.0824	1.0716
C7	H7A	0.9800	1.0954	1.0845
C7	H7B	0.9804	1.0910	1.0805
C7	H7C	0.9799	1.0894	1.0790
C8	H8A	0.9803	1.0962	1.0828
C8	H8B	0.9798	1.0925	1.0859
C8	H8C	0.9797	1.0950	1.0847

Table-7: Bond angles of 12-dimethyl-3-nitrobenzene in units of (°).

Atom 1	Atom 2	Atom 3	Angles		
			X-ray	DFT	HF
O1	N1	O2	123.34	124.15	124.41
O1	N1	C1	117.89	117.50	117.42
O2	N1	C1	118.73	118.34	118.16
N1	C1	C2	120.11	121.36	121.03
N1	C1	C6	115.80	115.32	115.30
C2	C1	C6	124.08	123.31	123.65
C1	C2	C3	116.18	116.64	116.61
C1	C2	C7	123.07	123.41	123.31
C3	C2	C7	120.73	119.94	120.07
C2	C3	C4	119.60	119.94	119.79
C2	C3	C8	121.08	121.09	121.27
C4	C3	C8	119.32	118.97	118.93
C3	C4	C5	122.23	121.83	121.96
C4	C5	C6	119.80	119.29	119.24
C1	C6	C5	118.08	118.97	118.72

Atomic net charges and molecular dipole moment

From the knowledge of the electron charge density function obtained after the multipolar refinement, one can easily derived the atomic and the molecular electrostatic properties.[24,25]The obtained components of the experimental molecular dipole moment are summarized in Table-9 and compared with the *ab initio* results for the isolated molecule. One can observe that there is no paradox between the resulting molecular dipole moment direction and the evaluation of the positive sign of the net charges on the H atoms and the negative sign of the net charges on the oxygen and nitrogen atoms. Atomic charges are

mostly used for the calculation of the charge distribution in a molecule.[26] The different net atomic charges are listed in Table-10 which gives also for a comparison the theoretical results. In this *ab initio* (B3LYP/6-31G*) procedure the treatment is confined to the valence-shell electrons. The results cited in Tables-9 and 10 show a good agreement between the values obtained by different methods. The dipole moment vector depends mainly on the position of substituents. The analysis of data led to dipole moment of 5 D and an orientation toward the dimethyl region as shown in Figure-7.

Table-8: Hydrogen bonds and their properties in 1,2-dimethyl-3-nitrobenzene crystal.

D–H…A	D–H/Å	D–A/Å	H–A/Å	D–H…A/Å	Type of bond	Properties
C7 -H7C ...O2	0.980	2.889	2.448	106.85	Intramolecular	Strong
C4 -H4 ...O2	0.950	3.608	2.716	156.70	Intermolecular	weak
C5 -H5 ...O1	0.950	3.710	2.818	156.74	Intermolecular	weak

Equivalent positions:

(0) x,y,z (1) -x+1/2+1,-y+1,+z-1/2 (2) x+1/2,-y+1/2+1,-z+1

(3) -x+1,+y-1/2,-z+1/2+1 (4) -x,+y-1/2,-z+1/2+1 (5) x-1,+y,+z

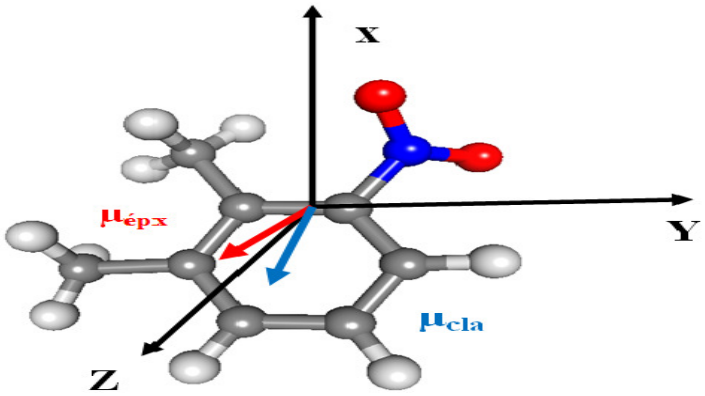

Fig.-7: Orientation of the molecular dipole moment of the title compound; the origin is at the centre of mass of the molecule; μ_{exp}: molecular dipole moment from the multipolar model; μ_c: molecular dipole moment from the ab initio calculation

Table-9: Components of the dipolar moment: X-ray experiment and theoretical ab initio calculations

Dipolar moment		μ_z(D)	μ_y(D)	μ_x (D)	μ_T (D)
Experimental		-4.9043	0.6517	-0.9005	6.5701
Theoretical	HF/6-31G**	-4.9041	0.7326	0.0498	4.9588
	B3LYP/6-31G**	-4.5498	0.3456	-0.0068	4.5629

Table-10: Net charges (q) in the different atoms of the title compound.

Atom	X-ray	DFT	HF
O1	-0.10086	-0.38429	-0.45477
O2	-0.10086	-0.38531	-0.44938
N1	-0.12358	-0.51249	0.44911
C1	0.02316	0.07072	0.13921
C2	-0.03203	0.00008	-0.01627
C3	-0.03203	-0.02128	-0.08201
C4	-0.04809	-0.20556	-0.10132
C5	-0.04809	-0.23411	-0.13406
C6	-0.04809	-0.21905	-0.06454

C7	-0.00122	-0.70823	-0.27285
C8	-0.00122	-0.70571	-0.30620
H4	0.08489	0.24215	0.13495
H5	0.08489	0.24932	0.14567
H6	0.08489	0.27117	0.17402
H7a	0.04304	0.26541	0.15898
H7b	0.04304	0.23994	0.12511
H7c	0.04304	0.26527	0.14488
H8a	0.04304	0.24653	0.12635
H8b	0.04304	0.24940	0.14190
H8c	0.04304	0.25107	0.14190

Electrostatic Potential

The electrostatic potential is used to distinguish electrophilic attack regions on the surface from nucleophilic attack ones.[27]The electrostatic potential around the molecule is obtained in a straightforward way from the charge density function produced in the non-spherical atom refinement. From the obtained continuous charge distribution at a point defined by *r'*, the potential is given by:

$$\phi(\mathrm{r}') = \int \frac{\rho_{total\,(\mathrm{r})}}{|r - r'|} dr \qquad (6)$$

In which ρ_{total} represents both the nuclear and the electronic charge. The integration is over the molecular volume and r represents the atomic position relative to common origin, the electrostatic potential distribution around the molecule obtained from the experimental X-ray diffraction data (a) and the *ab initio* theoretical calculations (b) are present in Figure-8. The obtained electrostatic potential as shown in figure undergoes the positive electrostatic potential around the 1-2-dimethyl and the H-benzene atoms sites while the negative electrostatic potential is located around the nitro group region. The good agreement between the experimental and the theoretical potential scheme was possible thanks to the special treatment accorded to the H atoms parameters derived from the multipolar refinement. In general the H positions are less accurate than desirable. Figure 8 also confirms the nature of the intramolecular charge transfer as determined by the orientation of the molecular dipole moment.

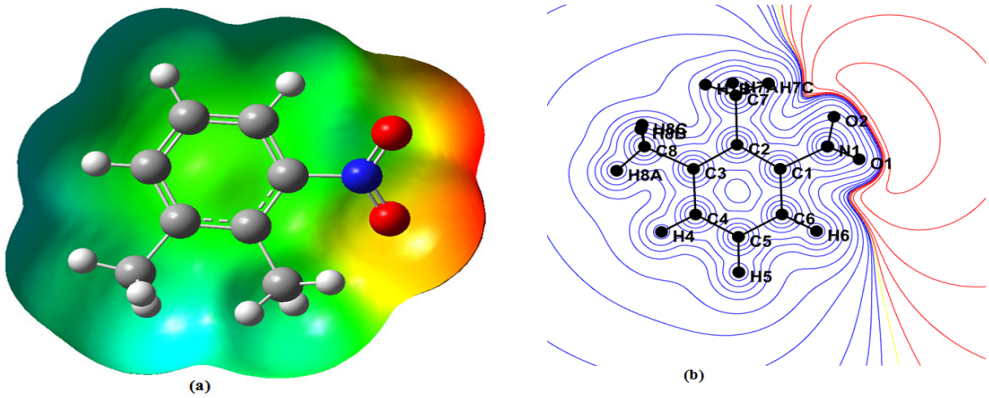

Fig.-8: The electrostatic potential maps around the title molecule;(a) *Ab initio* molecular orbital calculations of the electrostatic potential distribution; (b) Experimental electrostatic potential distribution predicted from X-ray diffraction data.

CONCLUSION

The introduced multipolar refinement model has significantly improved the structure refinement parameters. The final value of reliability factor decreased from 3.5 to 1 %. This testifies about the good quality of the used experimental data and the efficiency of the multipolar used model. The obtained

theoretical optimized bond lengths and bond angles are in good agreement with the corresponding experimental ones. So this study allowed us to extract a faithful description of the electron charge density distribution. However, no significant differences have been observed in the structural analysis of the molecule when using the multipolar Hansen-Coppens model. The most structural feature of the multipolar procedure is to give a better description of the H atoms parameters especially we have access to the anisotropic motion tensors as described in the rigid body bond test formalism. From the electron charge density function, a variety of dynamic density deformation maps has been drawn in which the accumulation of the electron charge density along the chemical bonding was shown clearly and was found almost centered in the middle of the chemical bonds. The oxygen free electron pairs were perfectly localized which allowed a better description of the intra (and inter) hydrogen bonding as shown in the topological analysis. The general conclusion from the estimation of the dipolar moments and the electrostatic potential of the 1,2-dimethyl-3-nitrobenzene molecule in the both experimental and theoretical study is that the region of the nitro group is electronegative and the dimethyl and H benzene atoms region is electropositive. Also the obtained orientation of the dipole moment shows clearly the direction of the intra charge transfer within the investigated molecule.

REFERENCES

1. N. Boukabcha, N. Benhalima, R. Rahmani, A. Chouaih and F. Hamzaoui, *Rasayan J. Chem.*, **8(4)**, 509(2015).
2. J. Shi Chun, F. Tai Yan and T. Liu Hong,*Bull. Korean Chem. Soc*., **34(11)**, 3485(2013)
3. C. K. Ingold, Structure and Mechanism in Organic Chemistry, 2nd ed.; Cornell University Press: Ithaca, New York, (1969)
4. H. A. Sparkes, H. J. Sageb and D. S. Yufitb, *ActaCryst. C*, **70**, 872 (2014).
5. N. K. Hansen andP. Coppens,*ActaCryst. A*,**34**, 909(1978)
6. K.N. Trueblood, Program THMAI1, Los Angeles: Department of Chemistry and Biochemistry, University of California, (1990)
7. F. L. Hirshfeld,*ActaCryst. A*,**32**, 239(1976)
8. A. D. Becke, *J. Chem. Phys*.,**98**, 5648(1993)
9. C. Lee, W. Yang andR. G. Parr, *Phys. Rev. B*,**37**, 785(1988)
10. H. D. Cohen andC. C. J. Roothaan, *J. Chem. Phys*., **43**, S34(1965)
11. G. Rauhut andP. Pulay, *J. Phys. Chem*., **99**, 3093(1995)
12. A. C. Gómez Marigliano andE. L. Varetti, *J. Phys. Chem*. A,**106**, 1100(2002)
13. Y. Dimitrova andJ. A. Tsenov, *SpectrochimicaActa Part A*, **68**, 454(2007)
14. F. Sim, A. St.-Amant, I. Papai andD. R. Salahub, *J. Am. Chem. Soc*., **114**, 4391(1992)
15. Gaussian 09, Revision B.01, Gaussian Inc., Wallingford CT, (2010).
16. A. Frisch, A.B. Nielsen and A.J. Holder, Gaussview Users Manual, Gaussian Inc., Pittsburgh, (2007).
17. P. Coppens, X-ray Charge Densities and Chemical Bonding,Oxford, New York, (1997)
18. C. Jelsch, B. Guillot, A. Lagoutte andC. Lecomte,*J. Appl. Crystallogr*.,**38(1)**, 38(2005)
19. F.L. Hirshfeld, *Acta Cryst. B*,**27**, 769(1971)
20. F.L. Hirshfeld,*Theor. Chim. Acta*,**44**, 129(1977)
21. F.L. Hirshfeld and H. Hope,*Acta Cryst. B*,**36**, 406(1980)
22. F. Baert, P. Schweiss, G. Heger and M. More,*J. Mol. Struct*.,**178**, 29(1988)
23. B. Guillot, *Acta Cryst. A*,**67**, C511 (2011)
24. N. Boubegra, A. Chouaih, M. Drissi and F. Hamzaoui,*Chin. Phys. B*,**23(1)**,000001(2014)
25. Y. Megrouss, N. Benhalima, A. Chouaih, N. Boukabcha, R. Bahoussi andF. Hamzaoui,*Chin. Phys. B*,**24(10)**, 106103(2015)
26. G. Raja, K. Saravanan and S. Sivakumar, *Rasayan J. Chem*., **8(1)**, 8(2015)
27. T. Chithambarathanu, K. Vanaja and J. Daisy Magdaline, *Rasayan J. Chem*., **8(4)**, 490(2015)

[RJC-1474/2016]